catalysts

Supplementary Information

Vanadium Complexes Derived from *O*,*N*,*O*-tridentate 6-bis(*o*-hydroxy-alkyl/aryl)pyridines: Structural Studies and Use in the Ring-Opening Polymerization of ε-Caprolactone and Ethylene Polymerization

Mark R. J. Elsegood [1], William Clegg [2] and Carl Redshaw [3,*]

[1] Chemistry Department, Loughborough University, Loughborough, LE11 3TU, UK; m.r.j.elsegood@lboro.ac.uk
[2] Chemistry, School of Natural & Environmental Sciences, Newcastle University, Newcastle upon Tyne NE1 7RU, UK; bill.clegg@ncl.ac.uk
[3] Plastics Collaboratory, Chemistry, School of Natural Sciences, University of Hull, Cottingham Road, Hull HU6 7RX, UK
* Correspondence: c.redshaw@hull.ac.uk

Contents:

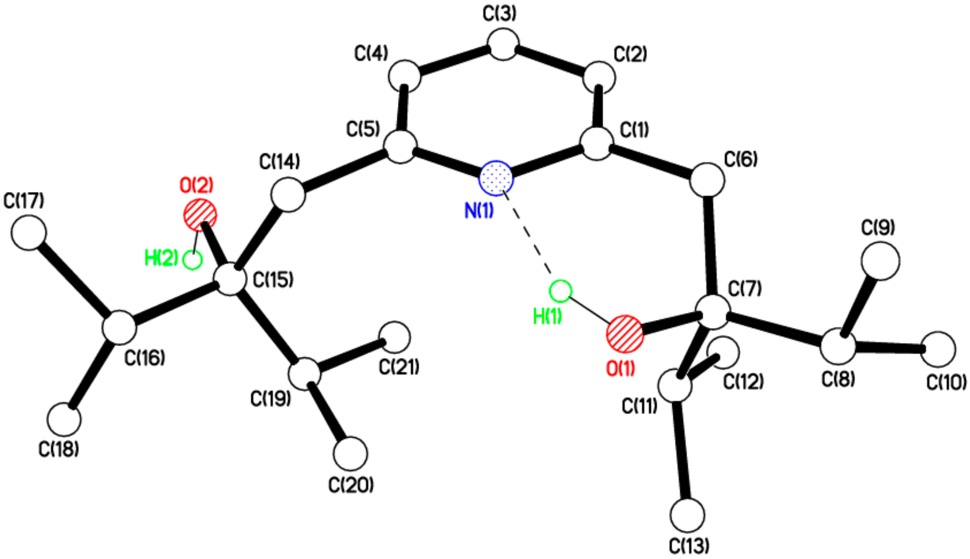

Figure S1. Molecular structure of L^1H_2. There is one molecule in the asymmetric unit.

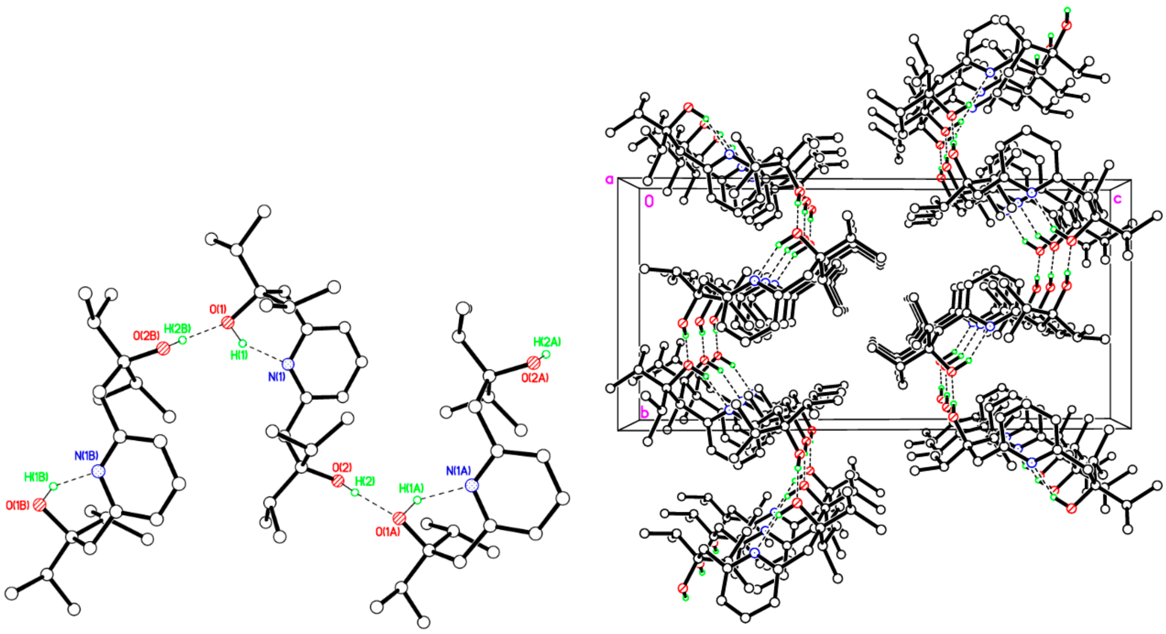

Figure S2. Intermolecular interaction and packing of L^1H_2. Intramolecular O–H···N H-bond from one hydroxyl group {at O(1)} to the pyridyl nitrogen with an S(6) motif. The other hydroxyl, at O(2), forms an intermolecular H-bond to a hydroxyl oxygen of the first type on a neighbouring molecule in the *b* direction with a C(8) motif.

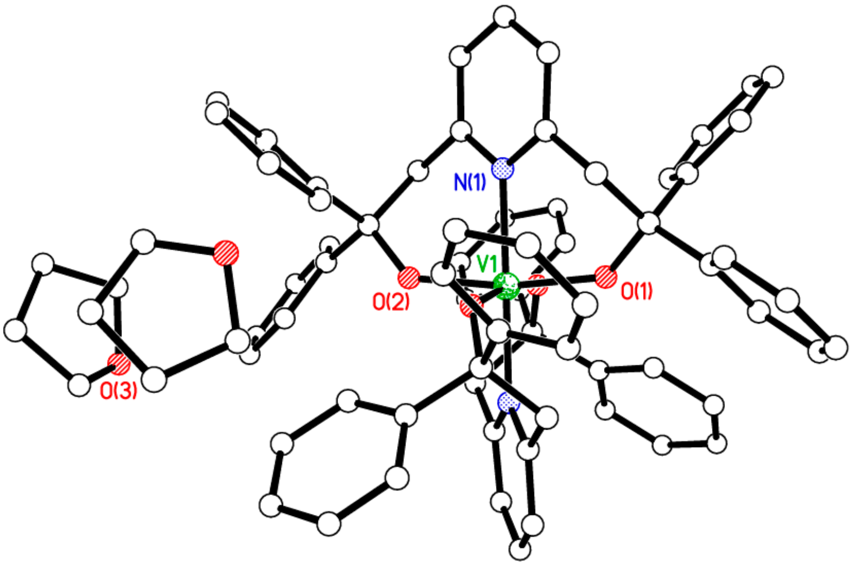

Figure S3. Alternative view of the molecular structure of [V({OC(Ph)$_2$CH$_2$}$_2$(*trans*-NC$_5$H$_3$))$_2$]·2THF (**3**·2THF).

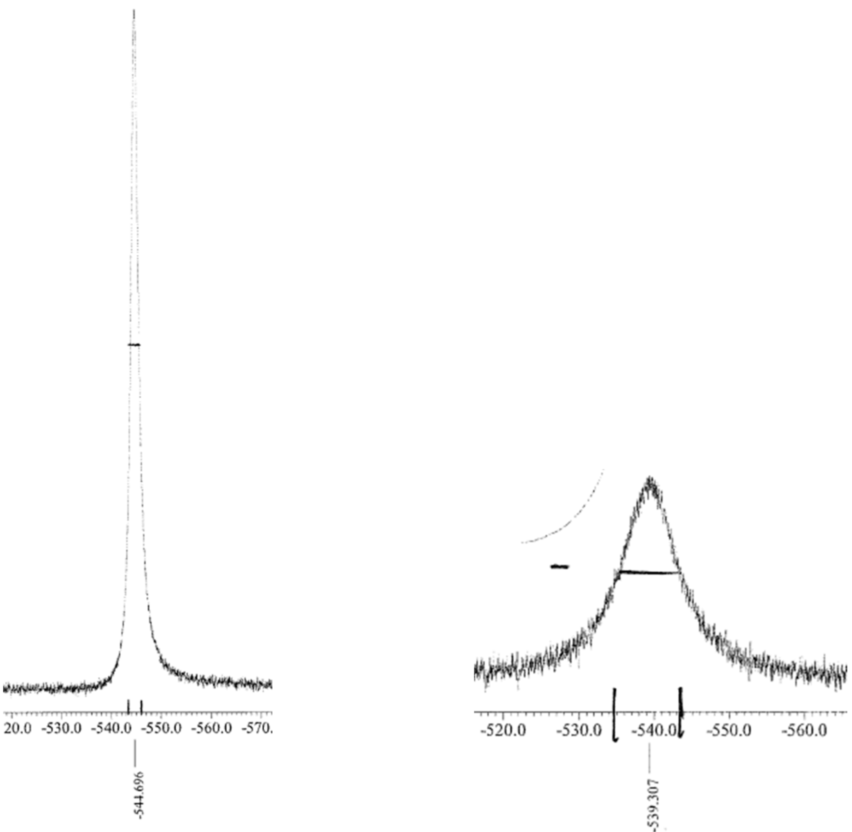

Figure S4. Example ^{51}V NMR spectra (105.1 MHz in C_6D_6, 298K). Left of **4**; right of **6**.

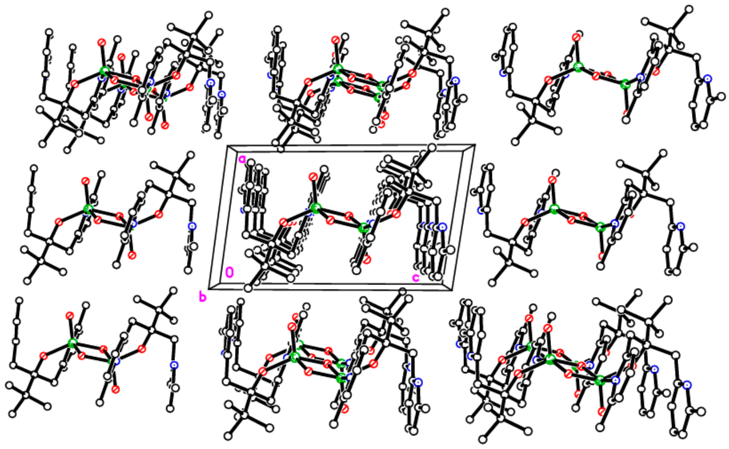

Figure S5. Packing in **6**.

X-ray Crystallography.

Diffraction data were collected on CCD or pixel array detector-equipped diffractometers using rotating anode or sealed tube (for **3**) X-ray sources. Data were corrected for absorption, polarisation and Lp effects. All of the structures were solved and refined routinely. [1,2] H atoms were included in a riding model except the O*H* in L^1H_2 which was freely refined. CCDC 2239107-2239113 contain the supplementary crystallographic data for this paper. These data can be obtained free of charge from The Cambridge Crystallographic Data Centre via www.ccdc.cam.ac.uk/structures.

Table S1. Crystallographic data for **1**, **2** and **3**·2THF.

Compound	**1**	**2**	**3·2THF**
Formula	$C_{36}H_{34}NO_4V$	$C_{66}H_{54}N_2O_4V$	$C_{74}H_{70}N_2O_6V$
Formula weight	595.58	990.05	1134.26
Crystal system	Monoclinic	Monoclinic	Monoclinic
Space group	$P2_1/n$	$P2_1/n$	$I2/a$
Unit cell dimensions			
a (Å)	14.1682(6)	13.53275(12)	19.534(2)
b (Å)	11.8251(4)	19.22120(15)	15.4318(18)
c (Å)	18.9210(9)	19.65243(19)	19.863(2)
α (º)	90	90	90
β (º)	105.054(5)	96.6467(8)	101.337(2)
γ (º)	90	90	90

V (Å^3)	3061.2(2)	5077.55(8)	5870.8(11)
Z	4	4	4
Temperature (K)	100(2)	100(2)	160(2)
Wavelength (Å)	0.71073	1.54178	0.71073
Calculated density (g.cm^{-3})	1.292	1.295	1.283
Absorption coefficient (mm^{-1})	0.36	2.05	0.23
Transmission factors (min./max.)	0.458 and 1.000	0.900 and 1.000	0.841 and 0.897
Crystal size (mm^3)	0.11×0.09×0.01	0.07×0.04×0.04	0.25×0.24×0.12
θ(max) (°)	29.6	70.4	28.5
Reflections measured	38147	91091	18019
Unique reflections	8501	9641	6711
R_{int}	0.112	0.042	0.045
Reflections with $F^2 > 2\sigma(F^2)$	5759	8693	4534
Number of parameters	381	659	376
R_1 [$F^2 > 2\sigma(F^2)$]	0.056	0.035	0.048
wR_2 (all data)	0.143	0.092	0.120
GOOF, S	1.02	1.04	1.02
Largest difference peak and hole (e Å^{-3})	0.68 and –0.64	0.30 and –0.57	0.33 and –0.42

Table S2. Crystallographic data for **4 – 6** and L^1H_2

Compound	**4**	**5**	**6**	$\mathbf{L^1H_2}$
Formula	$C_{24}H_{42}NO_4V$	$C_{24}H_{42}NO_4V$	$C_{38}H_{50}N_4O_6V_2$	$C_{21}H_{37}NO_2$
Formula weight	459.52	459.52	760.70	335.51
Crystal system	Monoclinic	Orthorhombic	Triclinic	Monoclinic
Space group	$P2_1/n$	$Pca2_1$	$P\bar{1}$	$P2_1/c$
Unit cell dimensions				
a (Å)	10.84157(10)	15.66703(12)	7.91377(17)	7.5267(2)
b (Å)	17.60523(18)	20.25108(14)	9.1860(3)	11.4467(3)
c (Å)	12.79976(12)	15.73473(11)	13.0852(3)	23.4237(6)
α (º)	90	90	83.710(2)	90
β (º)	96.7571(9)	90	80.7205(18)	93.094(2)
γ (º)	90	90	78.802(2)	90
V (Å^3)	2426.10(4)	4992.23(6)	917.91(4)	2015.15(9)
Z	4	8	1	4
Temperature (K)	100(2)	100(2)	100(2)	100(2)
Wavelength (Å)	1.54178	1.54178	1.54178	1.54178
Calculated density (g.cm^{-3})	1.258	1.223	1.376	1.106
Absorption coefficient (mm^{-1})	3.64	3.54	4.68	0.54
Transmission factors (min./max.)	0.553 and 1.000	0.702 and 1.000	0.712 and 1.000	0.922 and 0.986
Crystal size (mm^3)	0.30×0.18×0.03	0.24×0.14×0.02	0.12×0.08×0.02	0.21×0.10×0.03
θ(max) (°)	70.1	68.2	68.2	76.8
Reflections measured	37710	52150	22171	19710
Unique reflections	4601	8652	3232	4047
R_{int}	0.048	0.031	0.025	0.048
Reflections with $F^2 > 2\sigma(F^2)$	4458	8347	3232	3343

Number of parameters	281	561	231	233
R_1 [$F^2 > 2\sigma(F^2)$]	0.032	0.027	0.023	0.052
wR_2 (all data)	0.089	0.075	0.066	0.152
GOOF, S	1.06	1.10	1.08	1.05
Largest difference peak and hole (e Å^{-3})	0.45 and –0.43	0.17 and –0.32	0.31 and –0.32	0.32 and –0.23

Ring opening polymerization

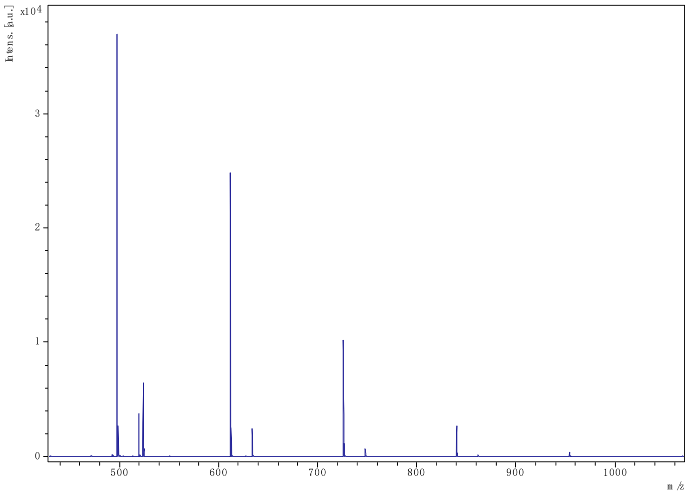

Figure S6. MALDI-ToF spectrum of PCL using **5** under N_2 at 70 °C (entry 14, Table 1). Present are a major family including chain oligomers terminated by 2 OH [M = 17 (OH) + 1(H) + n × 114.14 (CL) + 22.99 (Na^+)] (e.g. peak 612 = (5 × 114.14) + 23 + 18; 726 (6 × 114.14) +23 + 18).

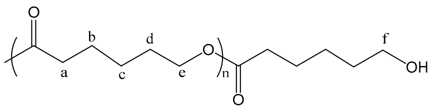

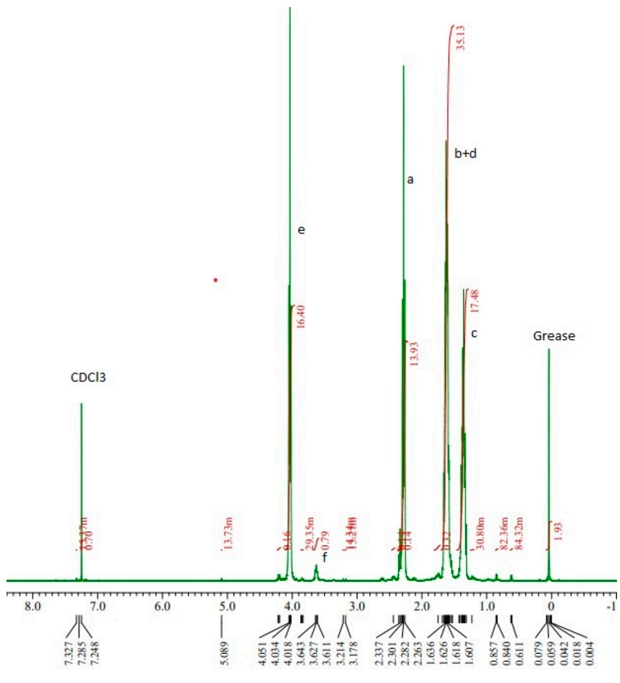

Figure S7. ^{1}H NMR spectrum of PCL (using **1** in air, entry 5, Table 1).

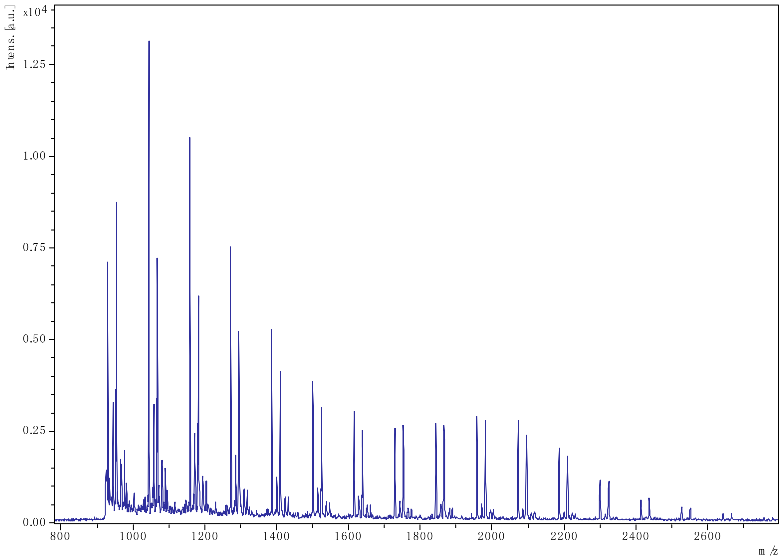

Figure S8. MALDI-ToF spectrum of PCL using **1** under air (entry 5, Table 1). Present are a number of families including chain polymers terminated by 2 OH [M = 17 (OH) + 1(H) + n × 114.14 (CL) + 22.99 (Na^+)] (e.g. peak 1753 = (15 × 114.14) + 23 + 18), as well as by the pyridine phenol/phenolate and OH [M = 470.6 ($C_{33}H_{28}NO_2$) + 1(H) + n × 114.14 (CL) + 22.99 (Na+)] (e.g. peak 2207 = (15 × 114.14) + 23 + 471.6).

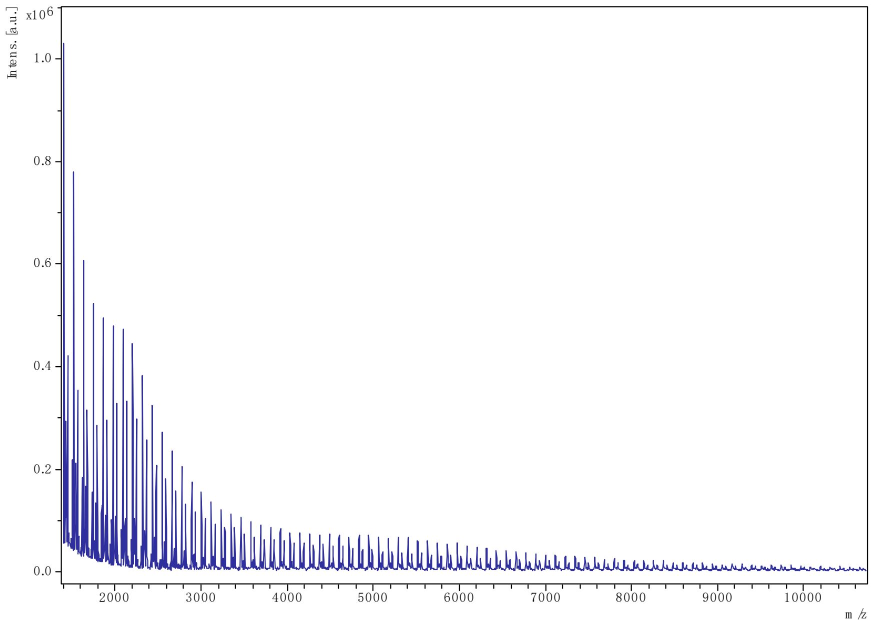

Figure S9. MALDI-ToF of PCL obtained using **5** under N_2 as a melt (entry 7, Table 2). Present are chain polymers terminated by 2 OH [M = 17 (OH) + 1(H) + n × 114.14 (CL) + 22.99 (Na^+)] (e.g. peak 1753= (15 × 114.14)+23+18), terminated by OH/O*i*Pr [M = 59 (OC_3H_7) + 1(H) + n × 114.14 (CL) + 22.99 (Na^+)] (e.g. peak 4648 = (40 × 114.14)+23+60), and cyclic polymers [M = 22.99 (Na^+) + n × 114.14 (CL)] (e.g. peak 1735 = (15 x 114.14) + 23).

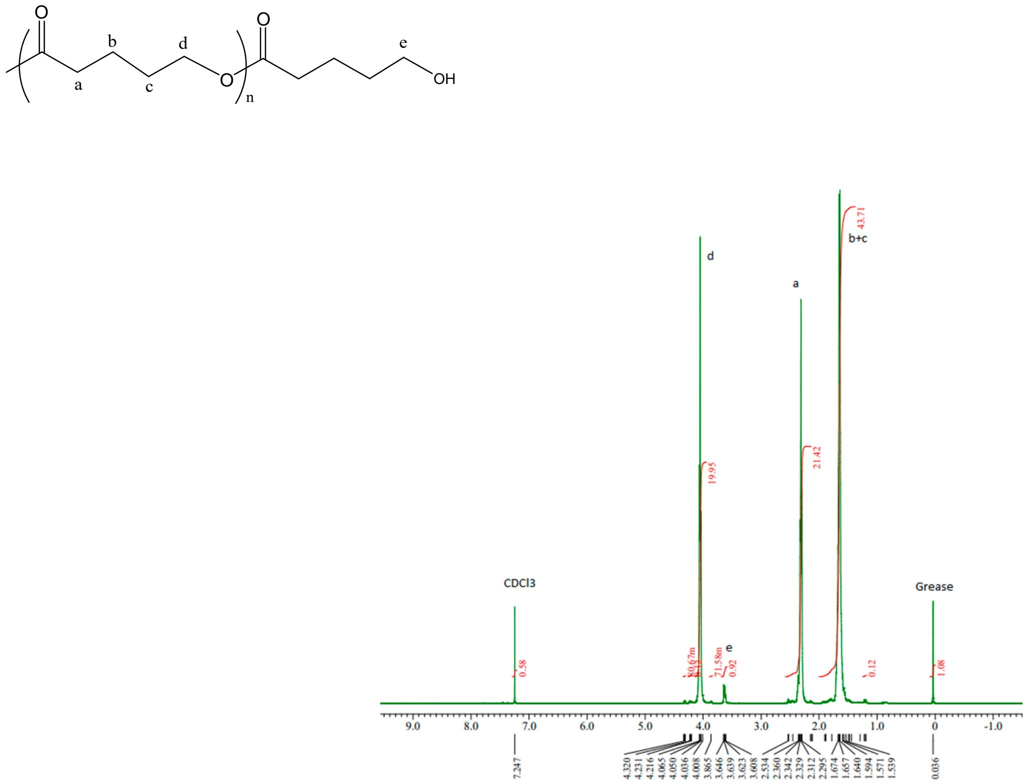

Figure S10. [1]H NMR spectrum of PVL (using **4** under N_2, entry 6, Table 3).

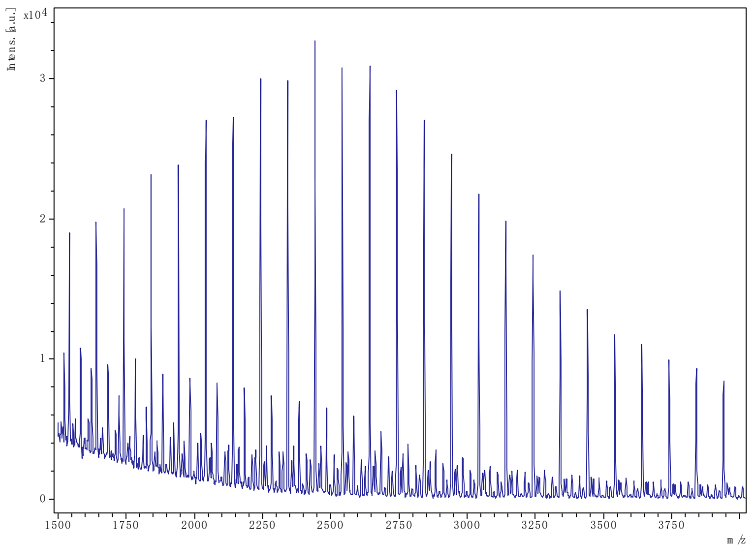

Figure S11. MALDI-ToF spectrum of PVL using **5** as a melt under N_2 (entry 8, Table 3). Present are chain polymers terminated by OH/O*i*Pr [M = 59 (OC_3H_7) + 1(H) + n × 100.12 (VL) + 22.99 (Na^+)] (e.g. peak 2085 = (20 × 100.12) + 23 + 60), and cyclic polymers [M = 22.99 (Na^+) + n × 100.12 (VL)] (e.g. peak 1525 = (15 × 100.12) + 23).

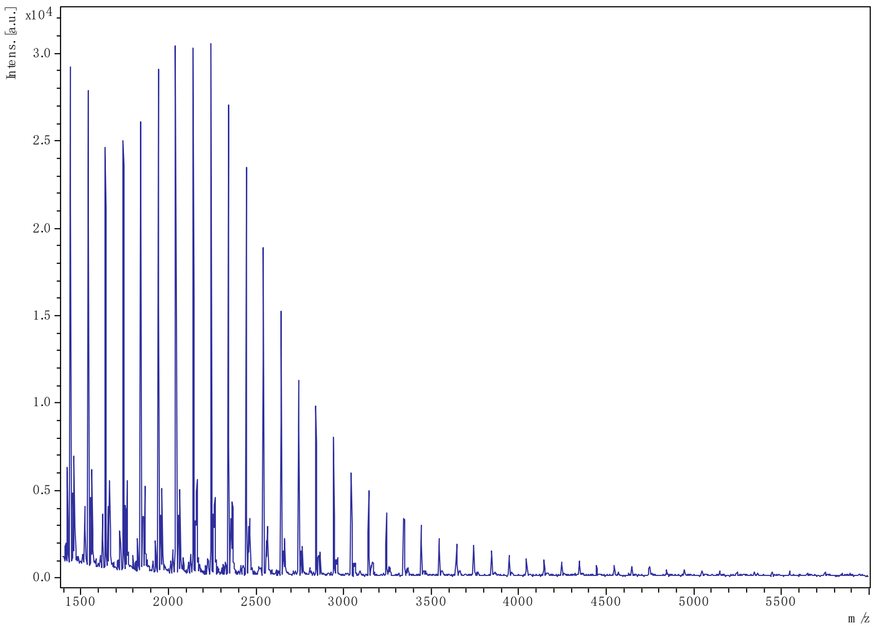

Figure S12. MALDI-ToF spectrum of PVL using **5** as a melt under air (entry 9, Table 3). Present are chain polymers terminated by 2 OH [M = 17 (OH) + 1(H) + n × 100.12 (VL) + 22.99 (Na^+)] (e.g. peak 1543 = (15 × 100.12) + 23 + 18), and a smaller series assigned to cyclic polymers [M = 22.99 (Na^+) + n × 100.12 (VL)] (e.g. peak 1525 = (15 × 100.12) + 23).

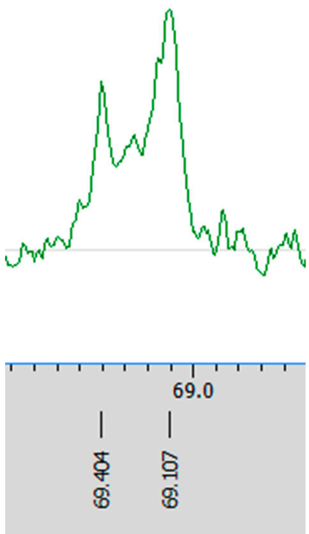

Pi = 1-2Iisi = 0.65

Figure S13. [13]C NMR spectrum of the methine region of the PLA using **6** under N_2 (entry 9, Table 4).

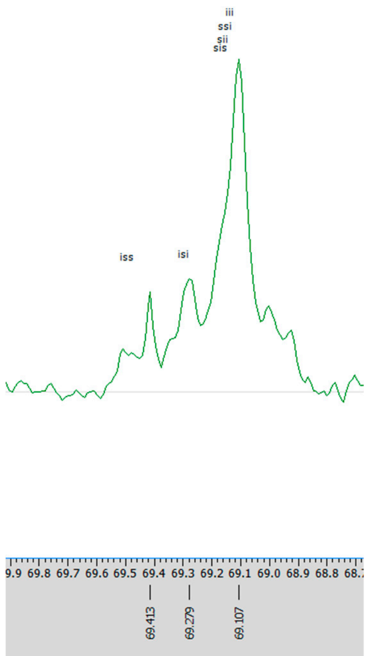

Pi = 1-2Iisi = 0.82

Figure S14. ^{13}C NMR spectrum of the methine region of the PLA using **6** under air (entry 10, Table 4).

References

1. G.M. Sheldrick, *Acta Cryst*. (2015), **A71,** 3-8.
2. G.M. Sheldrick, *Acta Cryst*. (2015), **C71,** 3-8